UNIVERSITY OF OSLO

FYS 3180/4180

H-11

Department of Physics

http://www.uio.no/studier/emner/matnat/fys/FYS3180/h11/

http://www.fys.uio.no/studier/kurs/fys3180/

Characterization of defects in proton-irradiated Si using deep level transient spectroscopy

Prosjektoppgave i FYS3180/4180, Fall-2011

Physical Electronics
Micro- and Nanotechnology Laboratory (MiNaLab)
University of Oslo

Abstract

In this investigation, dominant crystal defects in high purity silicon material subjected to proton irradiation will be studied using electrical measurement techniques, especially deep level transient spectroscopy (DLTS). The crystal defects are of point like nature, with an extension of a few Å to 1 nm, and the majority of the defects are of vacancy type. The positions in the energy band gap of the electron states caused by these defects will be determined as well as the kinetics of the thermal stability of the defects. Finally, on the basis of these results, the radiation hardness of the silicon material will be estimated and compared with requirements in high energy physics experiments at the Large Hadron Collider (LHC) at CERN and in satellite (space) experiments.

Content

I. Introduction

I.(a) Energy band structure and defect states in semiconductors

Semiconductor materials in use for electronic devices are normally crystalline in nature and the most common ones, like silicon (Si), germanium (Ge) and gallium arsenide (GaAs), all display a diamond structure. The diamond structure can be regarded as composed of two partially overlapping face centred cubic structures with a single atom at each lattice point. *Figure 1* shows an example for Si, which is the dominant semiconductor since more than 40 years. Between the lattice atoms and electrons there is a superposition of periodic Coulomb potentials from each lattice atom and the super-positioned potential exhibits the same periodicity as the crystal structure. This periodic potential lowers the total energy of the electrons in the crystal, leading to crystal binding, and the electrons are forced to assume certain energies only. More specifically, an energy interval with no electron states allowed emerges in materials with insulating and semiconducting properties. This energy interval is labelled the energy band gap (E_g) and is schematically illustrated in *Figure 2* ($E_g \approx 1.11$ eV for silicon at room temperature). The semi-infinite interval of energies with a lower limit at the upper edge of E_g is called the conduction band (E_c) and correspondingly, the energy interval with an upper limit at the lower edge of E_g is called the valence band (E_v).

In reality, any semiconductor is not perfect and will contain defects and impurities, either intentionally or unintentionally introduced. As a result, the crystalline periodicity is interrupted and energy states may appear within E_g, which affect the electrical properties of the semiconductor. A prime example is the introduction of group V impurities (P, As, Sb) or

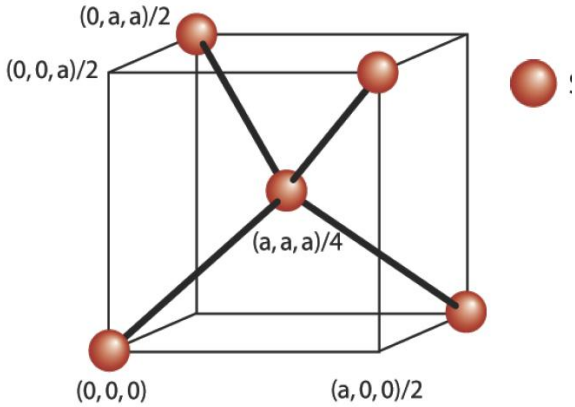

Figure 1. Tetrahedron formed by a Si-atom (centre) and the bonds to its four nearest neighbours.

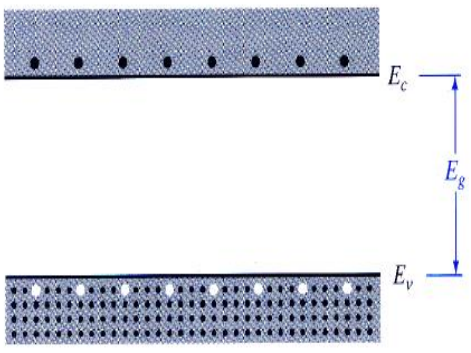

Figure 2. Simplified illustration of the energy band gap in a semiconductor[1]. Dark dots represent filled electron states and white dots show empty states (holes).

group III impurities (B, Al, Ga, In) on substitutional lattice sites in the silicon structure (so-called doping). The former ones will give rise to shallow electron states in E_g with respect to E_c and readily become positively ionized by thermal excitation of electrons to the almost empty conduction band (n-type doping). Correspondingly, the group III elements will cause shallow electron states in E_g with respect to E_v and readily become negatively ionized by thermal excitation of electrons from the almost fully occupied valence band (p-type doping). Consequently, the electrical conductivity of the Si material can be drastically changed, either by current transport via the almost free electrons in the conduction band (n-type conductivity) or via the valence electrons 'jumping' to nearby empty states, so-called holes (p-type conductivity)[1]. In addition, native (intrinsic) crystalline defects and unintentionally introduced residual impurities can appear in the material and some fundamental examples like vacancies and self-interstitials are schematically illustrated in *Figure 3*.

In silicon, the main residual impurities are oxygen, carbon and hydrogen[2]. Especially, oxygen can occur with high concentrations in as-grown single crystalline silicon material (~$1x10^{18}$ cm^{-3}, compared to the atomic density of ~$5x10^{22}$ cm^{-3}) and these oxygen atoms occupy normally a bond-centred interstitial configuration (O_i), as illustrated in some detail by *Figure 4(a).* The O_i atoms do not give rise to any energy state in E_g but they are likely to capture monovacancies (V's) in order to release the crystal strain associated with the O_i configuration. The resulting defect formed is shown in *Figure 4(b)* and is labelled the vacancy-oxygen (VO) centre[3]. The VO centre contains two dangling bonds from the two unsaturated Si atoms and an electron energy state appears at ~0.18 eV below E_c. Another prominent defect in silicon is the divacancy centre (V_2)[4] which consists of two V's in nearest neighbour lattice positions, as displayed in *Figure 4(c)*. The V_2 centre appears in particular after a silicon material has been exposed to irradiation with energetic particles, like protons and electrons in high energy physics experiments or in the Van Allen radiation belt,

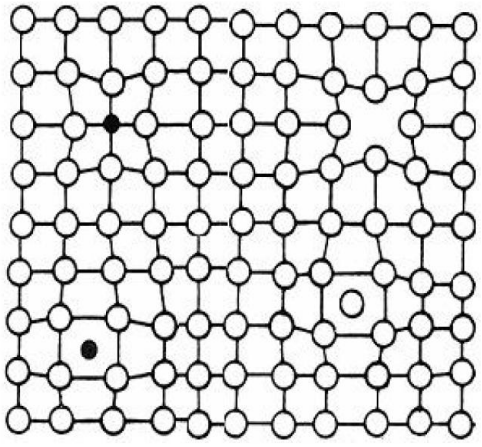

Figure 3. Illustration of fundamental point defects; vacancy (top right), self-interstitial (bottom right), substitutional impurity (top left) and interstitial impurity (bottom left). Open circles illustrate crystal host atoms and filled dark circles indicate impurity atoms.

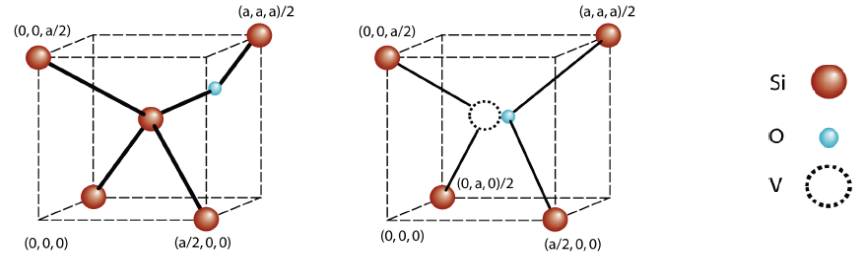

(a) The interstitial oxygen, O_i, is situated between two Si atoms.

(b) In the VO defect an O_i and a V share an Si substitutional site [1].

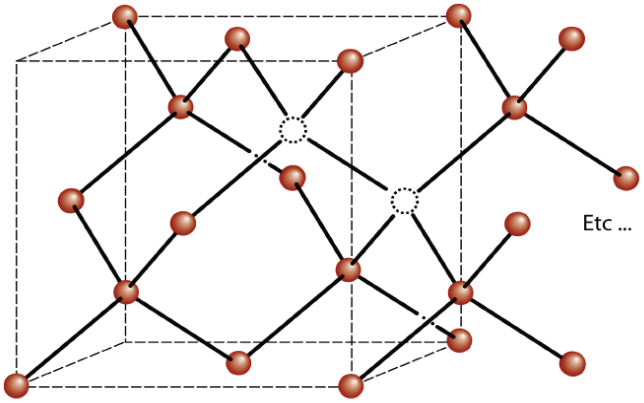

(c) V_2 is composed of two vacancies which are each others nearest neighbors and they each have three Si nearest neighbors [1].

Figure 4. Visualization of the atomic structure of the O_i (a), VO (b) and V_2 (c) defects.

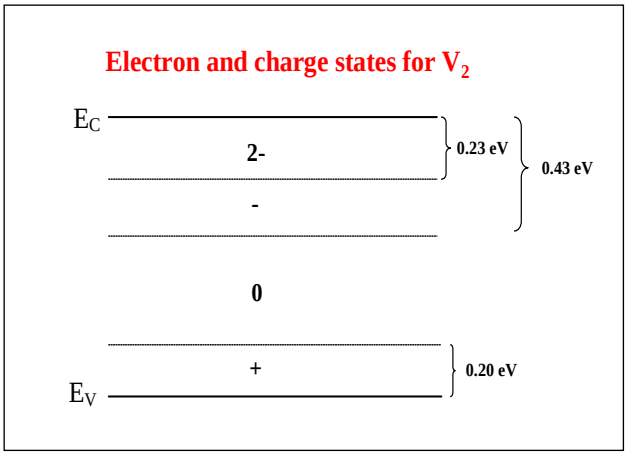

Figure 5. Illustration of electron states and charge states for the V_2 centre in silicon.

and it causes three different electron states in E_g corresponding to four charge states of V_2 (+, 0, -1, -2), as depicted in *Figure 5*.

I.(b) Emission and capture of electrons/holes by energy states in the band gap

Let us consider an electron state at an energy E_T below E_c and with a concentration of N_T. *Figure 6(a)* shows the total 'traffic' of electrons and holes to and from this state. The rate of emission of an electron to E_c and a hole to E_v are denoted by e_n and e_p, respectively. The rate of capture of an electron from E_c or a hole from E_v are nc_n and pc_p, respectively, where c_n and c_p are the so-called capture coefficients, and n and p are the concentrations of electrons in the conduction band and holes in the valence band, respectively.

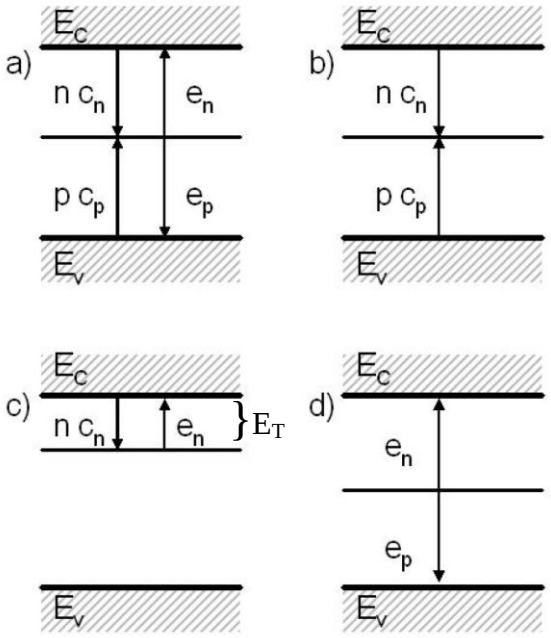

Figure 6. The total 'traffic' of charge carriers to and from a state is shown in (a). The special case of recombination is given in (b), trapping and emission in (c), and generation in (d).

Three typical situations can be identified; first, as shown in *Figure 6(b)*, a state may act as a recombination centre for pairs of electrons and holes. Second, as shown in *Figure 6(c)*, a state can act as a trap, and trapping and emission of electrons (or holes) are the dominating processes. Third, as shown in *Figure 6(d)*, a state can act as a generation centre for pairs of electrons and holes.

According to Shockley and Read[5], the capture coefficient for a state can be expressed as:

$$c_{n(p)} = \sigma_{n(p)} v_{th}$$

where $\sigma_{n(p)}$ is the capture cross section for electrons (holes) and v_{th} is the thermal velocity,

$$v_{th} = (3kT/m^*_{n(p)})^{½}$$

with $m^*_{n(p)}$ as the effective mass for electrons (holes), T as the absolute temperature, and k as Boltzmann's constant.

For the emission rate, the following relation holds[5]:

$$e_{n(p)}(T) = v_{th}\, \sigma_{n(p)} N_{C(V)} \exp(-E_T/kT) \qquad (1)$$

where $N_{C(V)}$ is the effective density of states in the conduction (valence) band.

II. Experimental

II.(a) Sample analysis by deep level transient spectroscopy (DLTS)

DLTS is the main technique to be used for the sample analysis, and in this section a brief introduction to the basic principles of DLTS is given. The technique was first introduced by Lang in 1974[6] and from DLTS one can obtain information about energy positions of states in the band gap, capture cross sections for electrons and holes, average concentration of energy states (defects) as well as concentration-versus-depth profiles of the states. In particular, a hallmark of DLTS is a very high sensitivity reaching detection limits on the order of 10^{-5} relative to the doping concentration.

DLTS requires a good rectifying junction in a semiconductor material, either a pn-junction or a Schottky barrier junction, and it is based on measurements of the junction capacitance. The basic structure of a pn-junction is given in *Figure 7*, and with the junction is associated a depletion region, W, which is depleted of free charge carriers (electrons and holes). As a result of W, a capacitance, C_r, builds up at the junction and is given by

$$C_r = \frac{\varepsilon A}{W} \qquad \text{with } W = \sqrt{\frac{2\varepsilon V_r}{q}\left(\frac{1}{N_a} + \frac{1}{N_d}\right)}$$

where ε is the permittivity (dielectric constant) of the material, A is the diode area, V_r is total bias over the junction, q is the elementary charge, N_a is the acceptor doping concentration and N_d is the donor concentration.

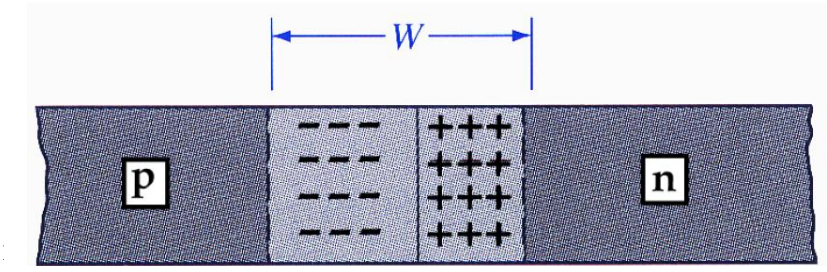

Figure 7. Schematics of a pn-junction showing the ionized N_a^- and N_d^+ dopants in the p- and n-regions, respectively. W denotes the depletion region.

In practice, an asymmetrically doped junction, like p^+n ($N_a >> N_d$) or a Schottky junction, is normally used for DLTS measurements and for a p^+n-junction C_r is simplified to

$$C_r = A\sqrt{\frac{\varepsilon q N_d}{2V_r}}.$$

In accordance with section I.(b), let us consider an electron state in the upper half of E_g with a position of E_T below E_c, as shown in *Figure 6(c)*, and a concentration of N_T. In DLTS, the capacitance is measured during pulsing of the junction voltage and a measurement sequence is illustrated in *Figure 8*. In *Figure 8(a)*, the junction is kept at reverse bias and the electron state is empty in the depletion region. In *Figure 8(b)*, a voltage pulse is applied and the reverse bias is reduced; as a result, the width of W decreases and the electron state can capture electrons provided that the duration of the pulse is sufficiently long. In *Figure 8(c)*, the voltage

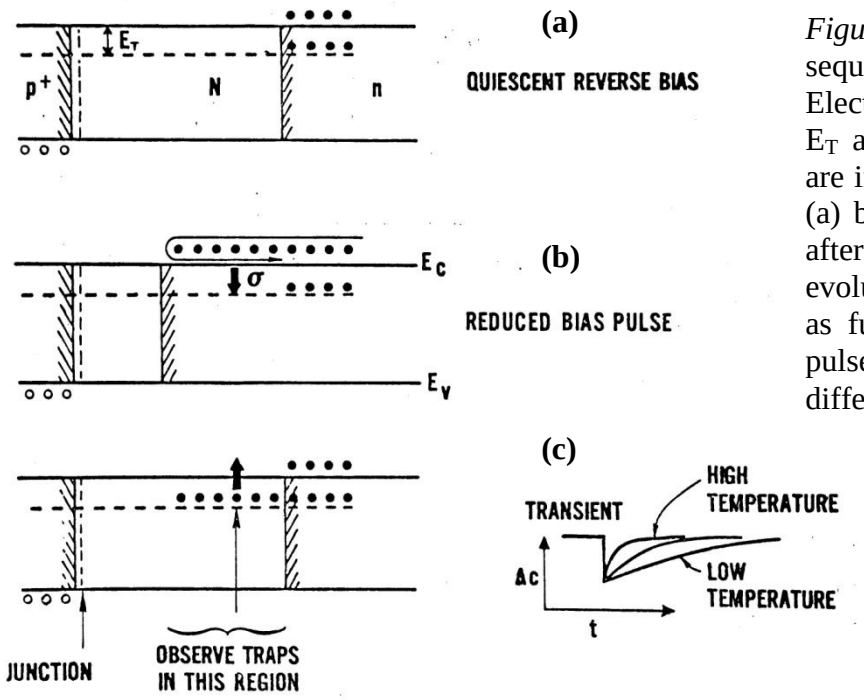

Figure 8. DLTS voltage pulse sequence for a p^+n junction. Electron occupation of state E_T and depletion layer width are indicated corresponding to (a) before, (b) during and (c) after the pulse. In (c), also the evolution of the capacitance as function of time after the pulse removal is indicated for different temperatures.

pulse is removed and V_r returns to its value in *Figure 8(a)*. After removing the pulse in *Figure 8(c)*, the effective doping concentration, N_d^{eff}, in W is given by

$$N_d^{eff} = N_d - n_T(t)$$

where

$$n_T(t) = N_T \exp(-e_n t).$$

The quantity $n_T(t)$ represents the concentration of filled electron states as a function of time, *t*, after the pulse removal. The expression above for $n_T(t)$ can be derived from Shockley-Read-Hall statistics[5] and shows that the emptying of the electron states is a thermally activated process with a rate constant equal to e_n (given by *Equation (1)*) and an exponential time dependence.

Hence, the capacitance after removing the pulse becomes

$$C(t) = A\sqrt{\frac{\varepsilon q N_d^{eff}}{2V_r}} = A\sqrt{\frac{\varepsilon q(N_d - n_T(t))}{2V_r}}$$

and assuming $N_T << N_d$ one obtains:

$$C(t) = C_r - \Delta C(t)$$

where

$$\Delta C(t) = \frac{C_r N_T}{2N_d} \exp(-e_n t).$$

The recovery of the capacitance as a function time occurs faster with increasing temperature, as illustrated in *Figure 8(c)*, and by taking the difference between $C(t_1)$ and $C(t_2)$ as a function of temperature a DLTS spectrum is obtained, *Figure 9*. A maximum in the DLTS signal occurs when the time interval $t_2 - t_1$ is on the order of the inverse rate constant $(e_n)^{-1}$.

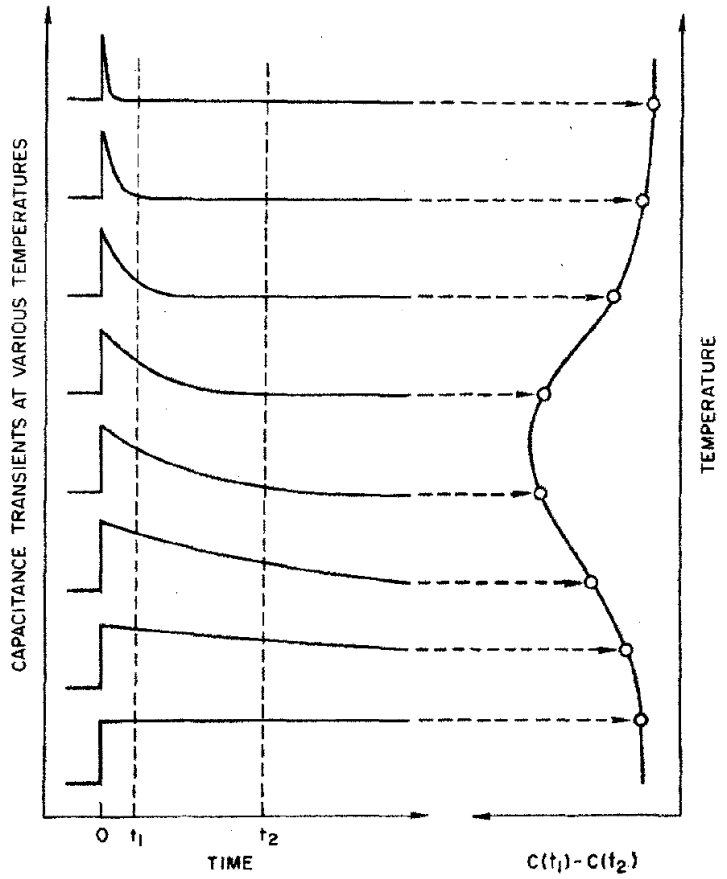

Figure 9. Illustration of how a DLTS spectrum can be obtained. The left hand side shows $C_r + \Delta C(t)$ at various temperatures while the right hand-side shows the corresponding DLTS signal given by $C(t_1) - C(t_1)$ as a function of temperature.

In reality, the procedure outlined in *Figure 9* for extracting the DLTS signal is rather sensitive to noise in the capacitance measurements and instead, a sampling (weighting) function, $w(t)$, of the type shown in *Figure 10* is frequently used. This sampling function is of lock-in type and the DLTS signal, $S(t_i)$, is deduced according to

$$S(t_i) = \frac{1}{t_i}\int_{t_d}^{t_d+t_i} \Delta C(t) w(t) dt$$

where t_d is a delay time of the capacitance meter. For $t_d << t_i$, $S(t_i)$ has a maximum amplitude when

$$e_n t_i = 2.52$$

and the maximum value becomes

$$S_{max} = 0.102 \frac{C_r N_T}{N_d}.$$

Thus, N_T can be deduced from S_{max} and by varying t_i (the so-called time window) different values of e_n at the peak maximum are obtained versus temperature. Then, by applying *Equation (1)*, E_T and σ_n can be extracted using an Arrhenius plot provided that v_{th} and N_C are known.

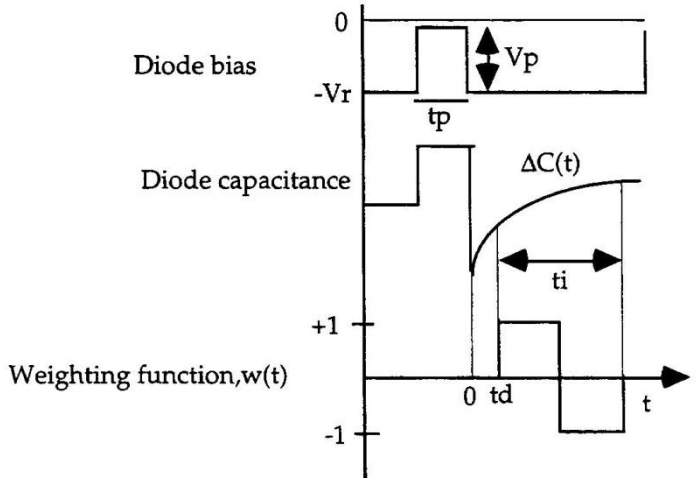

Figure 10. Illustration of $\Delta C(t)$ and the use of a sampling (weighting) function $w(t)$ of lock-in type.

II.(b) Samples to be studied

All the samples to be used in this study are cut from a silicon wafer having a highly n-doped (n^+) substrate with a lightly n-doped (n^-) epitaxial layer grown by chemical vapour deposition at ITME[7], see the schematic in *Figure 11(a)*. The wafers were subsequently processed by SINTEF/MiNaLab into pads of p^+-n^--n^+ diodes. The p^+-layer was realized by ion implantation of boron. The thickness of the epitaxial n^--layer is ~20 µm and the doping concentration, N_d, in the layer is about $3x10^{13}$ cm^{-3}.

After processing, rectangular samples with a size of about 2x2 mm^2 were cut form the wafers, and a photo of the processed and diced wafer is shown in *Figure 11(b)*.

Finally, the samples were irradiated with 1.5 MeV protons at room temperature to doses between $5x10^9$ and $6x10^{10}$ H^+/cm^2. The irradiations were undertaken at UiO/MiNaLab and the samples have then been stored in a freezer at -20 °C.

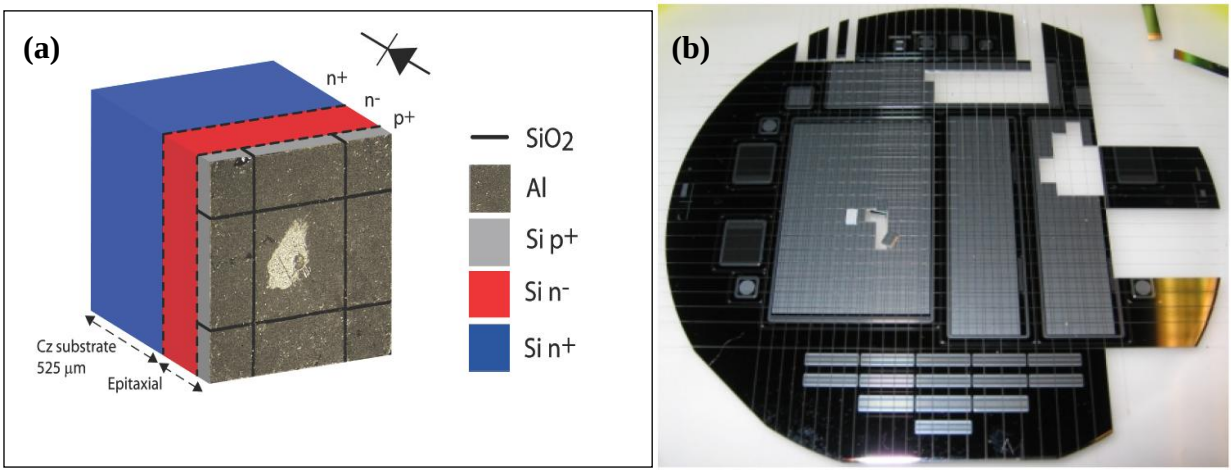

Figure 11. In (a), a schematic visualization of the p^+-n^--n^+ samples is given. The front contact is the middle square, isolated by dark ditches of silicon dioxide (SiO_2). The thickness of the epitaxial layer is about 20 µm with $N_d \approx 3x10^{13}$ cm^{-3}. The dimensions in (a) are not to scale. In (b), a photograph of a processed and diced wafer (∅ = 150 mm) is shown. The p^+-n^--n^+ samples can be seen as small $(2\ mm)^2$ squares located in the areas that are covered with aluminium (grey). The rest of the structures on the wafer are irrelevant for this investigation.

II.(c) Instrumentation for the measurements

The experimental setup to be used is designed for electrical measurements in the temperature range from 77 K (LN_2) to 400 K. The measurements include capacitance versus voltage and current versus voltage and spectroscopic techniques like DLTS,. A block diagram of the components in the setup and their interconnections is depicted in *Figure 12* together with a photograph of the sample cryostat. A core part of the setup is the capacitance meter (HP4280A) which enables recording of capacitance transients, $\Delta C(t)$, with a sampling rate of 1 MHz.

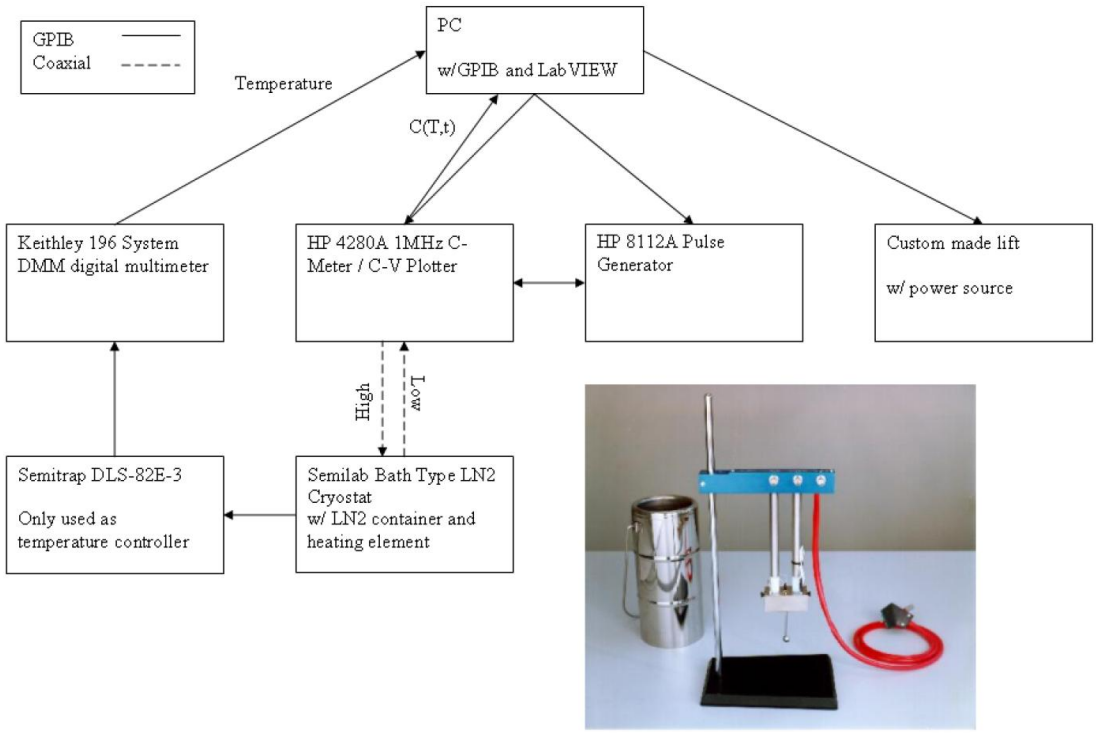

Figure 12. Block diagram of the DLTS setup to be used in this study. The photograph shows the sample cryostat and the LN_2 Dewar.

III. Definition of tasks

- Determine the energy position and electron capture cross section of the dominant electron states in the energy band gap of proton-irradiated high purity epitaxial silicon (n-type)
- Determine the concentration and generation rate of the dominant electron states as a function of proton dose
- On the basis of comparison with literature data, identify the origin of the dominant electron states
- Perform isothermal annealing studies to determine the thermal stability and annealing kinetics of the dominant electron states
- Conclude about the radiation hardness of the investigated samples (devices/detectors) and possibly predict their lifetime in (i) the Large Hadron Collider (LHC) at CERN and (ii) a satellite exposed to the Van Allen radiation belt.

IV. References

[1] B.G. Streetman and S. Banerjee, *Solid State Electronic Devices*, Prentice Hall International Inc., 6th edition (2006).

[2] See for example, M. Mikelsen, *Thermal evolution of irradiation induced defects in Silicon and Silicon Carbide*, PhD thesis, University of Oslo (2007), and references therein.

[3] J.W. Corbett, G.D. Watkins, R.M. Chrenko and R.S. McDonald, Phys. Rev. **121**, 1015 (1961); G.D. Watkins and J.W. Corbett, Phys. Rev. **121**, 1001 (1961).

[4] J.W. Corbett and G.D. Watkins, Phys. Rev. Lett. **7**, 314 (1961); G.D. Watkins and J.W. Corbett, Phys. Rev. **138**, A543 (1965).

[5] W. Shockley and W.T. Read, Phys. Rev **87**, 835 (1952).

[6] D.V. Lang, J. Appl. Phys. **45**, 3023 (1974).

[7] Institute of Electronic Materials Technology (ITME), Warszaw, Poland.